D2

Measuring human visual thresholds for sinusoidal gratings in an undergraduate class

B. Willmore* and D.J. Tolhurst†

** Psychology Department, UC Berkeley, CA 94720-1650 and †Department of Physiology, Downing Street, Cambridge CB2 3EG, UK*

It is fundamental to vision science to measure people's contrast thresholds for sinusoidal gratings or the responses of neurons in animals to gratings. Specialised graphics cards and displays costing thousands of pounds are needed for precise control of visual stimuli for research. Such costs are obviously prohibitive for teaching classes, but the psychophysics of grating thresholds allows excellent opportunities in the classroom to compare a person's overall visual performance with the behaviour of the neurons supposedly underlying that behaviour.

We have written a program in Microsoft Visual Basic to run under Microsoft Windows on relatively modest 'multimedia' PCs, which are already in our class for Histology teaching. Although stimulus definition in space and time is not perfect, we have good approximation to more 'professional' displays. Furthermore, students can get fairly reliable estimates of their contrast thresholds quickly; some 'professional' experimental protocols require 100 s of stimulus trials, and 40 minutes' concentration!

The observer faces the computer's monitor and sees two square panes side-by-side. Each pane is 4 degrees square when viewed from 114 cm. At first, the panes are uniform mid-grey. The experimenter starts a trial (using the mouse) and a 'movie' begins either in the left pane or the right, chosen randomly by the computer. The movie is of a sinusoidal grating whose contrast gradually increases from zero over several seconds. The observer looks rapidly to and fro between the two panes and, when a faint stimulus is first seen in one pane, he/she pushes left arrow or right arrow appropriately on the keyboard. The movie stops and, if the correct pane was chosen, the computer displays the contrast at which the movie was interrupted; the experimenter can plot that value directly onto graph paper. There is no explicit penalty for anticipating and choosing the wrong pane, apart from the scorn of the observer's peers! The protocol is quick and fairly reproducible; it appeals to the competitive instinct of some students.The gratings can be static or they can flicker at 5 Hz (180 deg phase-shift every 100 ms). Our displays have a frame rate of 60 Hz, and each 'movie' consists of 10 slightly different pictures per second. Under Microsoft Windows NT, we have not succeeded in synchronising the movie pictures exactly to the display frames. There are occasional glitches in movies of flickering gratings but these do not seem to detract.

Typically, computers display 256 grey levels, but we need many more than this to show the tiny nuances of luminance that compose a grating that is only just visible. Contrast thresholds can be less than 1 %. A crucial feature of our program is to extract over 3000 grey levels from the system; some of these are used to compensate for the nonlinear (roughly square-law) relation between the grey levels as calculated in the movie and the actual luminances on the display. The logical display resolution set by Windows must be the same as the physical pixel resolution of the display (1024 by 768 in our case) and the display set to '32 bit' colour. Each physical pixel can have 256 levels each of Red, Green and Blue (R, G and B), allowing 768 brightness levels (if we ignored colour). Starting from 'black', we could increment the brightness to 'bright white' by adding ones, in the sequence R-G-B-R-G-B-and so on; 2/3 of the brightness levels would not be precisely grey, and so it would be better to rearrange the RGB order every 3 grey levels. In fact, for moderate and low spatial frequencies, our movie frames are calculated with 128 by 128 logical pixels, but occupy 256 by 256 physical pixels on the display, each of which is less than 1 minute square. Then, each logical pixel occupies 4 physical ones, allowing a further factor of 4 in grey-level resolution. Increased grey levels are traded for decreased spatial resolution.

One can see how contrast thresholds for steady gratings depend upon spatial frequency: the pronounced low spatial-frequency cut supposedly shows lateral inhibition in the visual system or centre-surround antagonism of receptive fields. Flicker at 5 Hz shifts the sensitivity curve to low spatial frequencies, perhaps due to differences in the spatiotemporal preferences of P-and M-cells.

We can also examine 'masking'. Trials begin with the two panes containing identical, visible gratings. When the 'movie' runs, the contrast of the grating in one pane will increase slowly or a second grating will be added to the mask. Students can see the Weber-Fechner relationship for contrast discrimination. They can also look at the orientation specificity of masking, which may reflect the orientation selectivity of neurons in striate cortex.

All procedures accord with current local guidelines and the Declaration of Helsinki

D3

An inexpensive solid-state stimulator for ocular pursuit

R.H.S. Carpenter, M.F. Swann and S.J. Reitter

The Physiological Laboratory, University of Cambridge, Cambridge CB2 3EG, UK

In practical classes, and in some kinds of research, there is a need for a device that can display a target moving in a controlled manner, to evoke eye movements or other directed responses, without tying up an entire computer to do so. One obvious approach is to use a laser and voltage-driven mirror, but such systems are expensive and insufficiently robust to withstand much student use, and intrinsically limited in frequency response. What is needed is a compact device with no moving parts that can be controlled by an analogue signal, which in turn can be derived from a physiological recording system such as EPIC, or from a DAC connected to a USB or printer port.Whilst the new technologies using luminescent plastic appear promising, they are still expensive, the response-times can be long and the driving voltages needed to run them are difficult to generate.

Here we present a device using the very bright LEDs that are now available in micro-miniature, surface-mount form without individual diffusers or lenses (Infineon LSR976, 632 nm, 27mcd typical at the 8.5 mA used, 160° viewing angle). 128 such devices are arranged in a row, and individually driven with pulse-density modulation for control of brightness. Although the LEDs are close-packed (1.5 mm pitch), if the selector outputs were simply used to activate single LEDs the movement would appear jerky at slow scanning rates. For this reason, a high-frequency signal of small amplitude is added to the driving voltage, its waveform being such as to generate an approximately gaussian blur across a small number of the LEDs. The resultant voltage is digitised to 7 bits, the result then being sent to a 1/128 selector driving the LEDs. When the display is viewed through a mild diffuser, what is seen is a small spot of light, admittedly lacking sharp edges, but appearing to move smoothly even at the lowest velocities. The frequency response is absolutely flat in the range required (10 Hz at most), with complete linearity in terms of transverse distance.

D4

Dynamics of probability prediction in a saccadic latency task

Andrew J. Anderson and R.H.S. Carpenter

The Physiological Laboratory, University of Cambridge, Cambridge CB2 3EG, UK

The median time to make an eye movement to a suddenly appearing target (*saccadic latency*) depends upon a subject's expectation that the target will appear at a particular location. Previous work (Carpenter & Williams, 1995) found that, for fixed appearance probabilities, latency varies inversely with the log probability of a target's appearance. If the target's appearance probability changes, however, the subject's expectation must change as well. We investigated the time course of this expectation change.

We measured saccadic latencies in human subjects for runs of 200 sequentially presented targets, altering the left/right appearance probabilities at a random point between 70 and 120 presentations. Initial left/right probabilities were 0.5/0.5, altering to 0.1/0.9, 0.33/0.67, 0.5/0.5, 0.67/0.33 or 0.9/0.1. Targets were yellow light emitting diodes (LEDs), spaced six degrees either side of a central fixation LED, that appeared 0.5 to 1.5 seconds after the onset of the fixation LED. A computer system (Carpenter, 1994) determined saccadic latencies from the output of an infrared oculometer. By performing repeated measurements, we determined average latencies for each presentation relative to the change in probability. The procedures complied with the Declaration of Helsinki, and were approved by the local ethics committee.

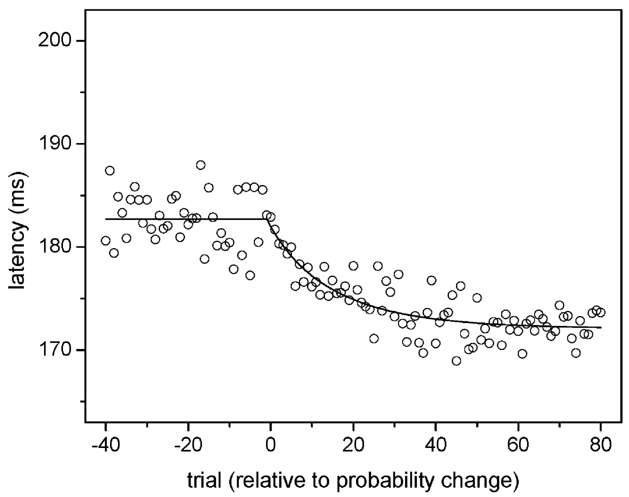

Figure 1. Mean latencies for left-going saccades to a target appearing on the left with an initial probability of 0.5 (trial < 0), changing to 0.9 (trial ⩾ 0). The line gives the maximum-likelihood fit of the model, where $\lambda = 0.05$ (slope and y-intercept for $\log(p_x)$ *vs.* latency are −42 and 169, respectively; goodness of fit Q = 0.4). The number of runs averaged was 110.

An abrupt change in appearance probability produced a continuous change in average saccadic latency that approached an asymptote (see Fig. 1). The continuous change commenced when the target probability changed, and was consistent with a 'forgetful' maximum-likelihood model that predicts:

$$p_x = (1\text{-}\lambda)p_x\text{-}1 + \lambda q$$

where p_x is the subjective probability estimate (or expectation) after x presentations, (1-λ) is the relative weighting given to the prior estimate of probability, and q is the probability that the target appeared in the location on presentation x. Latency should then be proportional to a logarithmic transform of p_x. The constant λ represents the trade-off between responding quickly to true probability shifts and not responding to normal variation at a fixed probability level, and was approximately 0.05 for our data. This constant has potential implications for survival, for which an organism must distinguish true change in the environment from normal stochastic variation.

Carpenter RHS & Williams MLL (1995). *Nature* **377**, 59–62.

Carpenter RHS (1994). *J Physiol* **480.P**, 4*P*.

All procedures accord with current local guidelines and the Declaration of Helsinki

C160

Characterisation of the electrogenic Na^+-Ca^{2+} exchange current in frog olfactory receptor cells

Salomé Antolin and Hugh R. Matthews

Physiological Laboratory, Downing Street, Cambridge CB2 3EG, UK

Ca^{2+} is a second messenger in olfactory receptor cells, important in their response and adaptation. Ca^{2+} enters through cyclic nucleotide-gated channels and is believed to leave via an exchange extrusion mechanism driven by the Na^+ gradient (Reisert & Matthews, 1998). To further characterise Na^+-Ca^{2+} exchange we have measured electrogenic currents associated with Ca^{2+} extrusion in isolated frog olfactory receptor cells.

Frogs, *Rana temporaria*, were killed by stunning then rostral and caudal pithing. The cell body of an isolated olfactory receptor cell was drawn into a suction pipette to measure currents flowing across the cilia, and the solution bathing the cilia rapidly exchanged by translating them between four flowing streams under computer control. To measure the electrogenic current associated with Na^+-Ca^{2+} exchange, the cilia were translated from normal Ringer to a solution in which guanidinium was substituted for Na^+ to incapacitate Ca^{2+} extrusion (Reisert & Matthews, 1998), which included 500 μM of the phosphodiesterase inhibitor IBMX to elevate the cAMP concentration within the cilia and allow loading with Ca^{2+} through the cyclic nucleotide gated channels. After 4 s, the cilia were translated for 2 s into a guanidinium-substituted solution without IBMX, to allow cAMP levels to fall and cyclic nucleotide-gated channels to close while maintaining Ca^{2+}_i at an elevated level; this solution included 1 mM niflumic acid to block the Ca^{2+}-activated Cl^- conductance. Then the cilia were returned to Ringer with 1 mM niflumic acid, allowing extrusion of the Ca^{2+} load. Junction currents between these solutions and Ringer in the suction pipette were corrected by subtraction of the currents obtained when the protocol was repeated in the absence of IBMX, thereby preventing Ca^{2+} loading.

Upon the return to Ringer after Ca^{2+} loading a decaying current was observed, which was not present in recordings without IBMX. In experiments for which the junction currents were stable throughout, the junction-corrected current could be fitted by a single exponential with a mean amplitude of 1.67 pA and a time constant of 1.22 ± 0.06 s (mean ± S.E.M.; $n = 11$ cells). The amplitude and time constant of this current were little affected by doubling the concentration of niflumic acid (2.09 pA, 1.56 ± 0.11 s; $n = 9$ cells), indicating that it was unlikely to represent residual unblocked Ca^{2+}-activated Cl^- current. This decaying component of current induced by the return to Na^+-containing solution after Ca^{2+} loading therefore appears to represent electrogenic Na^+-Ca^{2+} exchange in the olfactory receptor cilia.

Reisert J & Matthews HR (1998). *J Gen Physiol* **112**, 529–535.

This work was supported by the Wellcome Trust.

All procedures accord with current UK legislation

C161

Control by calcium of the rate-limiting step of phototransduction in red-sensitive salamander cones

Hugh R. Matthews * and Alapakkam P. Sampath †

** Physiological Laboratory, University of Cambridge, Downing Street, Cambridge CB2 3EG and †Department of Physiology and Biophysics, University of Washington, Seattle, WA, USA*

The shutoff of the phototransduction cascade in rod photoreceptors is dominated by a time constant of around 2 s (Pepperberg *et al.* 1992) which is unaffected by Ca^{2+}_i (Lyubarsky *et al.* 1996) and which may represent the hydrolysis by transducin of GTP (Sagoo & Lagnado, 1997). Instead, in rods, Ca^{2+}_i acts on a step early in phototransduction which takes place with a time constant of ~0.5 s (Matthews, 1997) which appears to represent rhodopsin quenching (Matthews *et al.* 2001). In contrast, response recovery in cones is poorly understood. We have therefore investigated the Ca^{2+}-dependence of the dominant time constant in salamander red-sensitive cones by rapidly superfusing the outer segment with a $0Ca^{2+}/0Na^{+}$ solution designed to minimise surface membrane Ca^{2+} fluxes, in order to delay the dynamic fall in Ca^{2+}_i which normally accompanies the flash response.

Aquatic tiger salamanders, *Ambystoma tigrinum*, were killed by stunning followed by decapitation and rostral and caudal pithing. Recordings were made from isolated red-sensitive cones drawn inner segment first into a suction pipette.

If the outer segment of a red-sensitive cone was stepped to $0Ca^{2+}/0Na^{+}$ solution just before a bright flash and returned to Ringer shortly before recovery then response saturation was prolonged in comparison to the response in Ringer, increasing linearly by 0.50 ± 0.07 (least squares regression, n = 9 cells) of the time spent in this solution. Furthermore, if the cone was pre-exposed to steady subsaturating light, thereby reducing Ca^{2+}_i, the prolongation of the bright flash response evoked by $0Ca^{2+}/0Na^{+}$ solution decreased progressively with increasing background intensity. These results resemble those obtained from rods which have been bleached and regenerated with 11-cis-9-demethylretinal, which prolongs Ca^{2+}-dependent photopigment quenching so that it dominates response recovery (Matthews *et al.* 2001). We therefore conclude that in cones the time constant that normally dominates response recovery is controlled by Ca^{2+}_i in a graded manner. During adaptation to steady light the accompanying fall in Ca^{2+}_i will act to accelerate the dominant time constant in cones, thereby contributing to the speeding of response recovery.

Lyubarsky A *et al.* (1996). *J Gen Physiol* **107**, 19–34.

Matthews HR (1997). *J Gen Physiol* **109**, 141–146.

Matthews HR *et al.* (2001). *J Gen Physiol* **118**, 377–390.

Pepperberg DR *et al.* (1992). *Vis Neurosci* **8**, 9–18.

Sagoo MS & Lagnado L (1997). *Nature* **389**, 392–395.

This work was supported by the Wellcome Trust.

All procedures accord with current UK legislation

C162

Does the short wavelength system contribute to human stereoscopic depth perception?

J. S. Lauritzen * and E. Negro †

** University of Ulster, Coleraine BT52 1SA, UK and † ESIL, Marseille, France*

The short wavelength branch of the visual system (SWS) has poor spatiotemporal resolution, and S-cones are more fragile, so that conditions like glaucoma selectively damage this branch of the visual system first. Psychophysical studies of the SWS in isolation can be carried out by adapting the L and M-cones with a yellow background, and presenting stimuli at the preferred wavelength of the S-cones.

We investigated whether people use information carried by the SWS to extract stereoscopic depth cues. Stimuli were displayed on a computer monitor with the red and green guns disabled. The entire apparatus was contained in a lightproof case with a viewing port at one end. A yellow adapting background could be interposed using a beam-splitter. Pictures of objects were viewed binocularly through LCD shuttered glasses, and could be displayed as page-flipped stereograms. This allowed 4 viewing conditions: non-adapted, no stereo display; yellow-adapted, no stereo display; non-adapted, with stereo display; and yellow-adapted, with stereo display. Three two-alternative forced-choice experiments, with feedback given after each trial, were carried out under the 4 viewing conditions. An experiment consisted of 20 presentations each of 10 different stimuli, presented in pseudorandom order:In experiment 1, subjects (n = 7) judged whether a wire frame box was taller or shorter than a perfect cube. This task requires a judgment based on 2D shape only. In experiment 2, subjects (n = 7) judged whether a wire-frame box was deeper or flatter than a perfect cube. This task uses a combination of 2D shape and stereo-cues. Experiments 1 & 2 used ten boxes deviating from a cube by ± 2–10 %. Lastly, subjects (n = 5) judged which of two solid spheres appeared closer to them. The spheres were offset by 5 to 25 voxels. The 2D outline of the two spheres was virtually identical for all trials, so that the task relied primarily on stereo-cues.

We found no significant differences between the viewing conditions in experiments 1 & 2 (thresholds ± S.E.M.: 2.2 ± 2.8 % deviation and 5.9 ± 1.2 % deviation; ANOVA, P = 0.99; P = 1.0), with neither the stereo-cues nor yellow-adaptation affecting performance. In experiment 3, there was a large difference between the stereo and non-stereo conditions, with subjects performing at chance for all levels of offset without the stereo-cues; there was good discrimination when stereo-cues were allowed ($P = 4.2\times10^{-4}$), and with significantly better performance when not adapted (threshold offset: yellow adapted: 13.1 ± 0.65 voxels, non-adapted: 7.6 ± 4.4 voxels; P = 0.013).

This suggests that the visual system does make use of SWS information for stereoscopic depth perception, although the lower spatial resolution of this system means that discrimination based on it is less accurate.

All procedures accord with current local guidelines and the Declaration of Helsinki

C163

Contrast masking and facilitation in human psychophysical experiments using natural scene stimuli

M. Chirimuuta and D.J. Tolhurst

Department of Physiology, University of Cambridge, Cambridge CB2 3EG, UK

It has repeatedly been observed (e.g. Foley 1994) that the minimum detectable contrast difference of a sinusoidal grating is a function of the base contrast of the grating. For low contrast gratings, the discrimination threshold drops below the detection threshold (facilitation effect) and rises as base contrast increases (masking effect). This pattern of results is known as the dipper function. We present the results of two observers for psychophysical contrast discrimination experiments that used natural images, rather than sinusoidal stimuli.

Stimuli were two digitised, linearised black-and-white photographs of natural scenes, and two random dot patterns that were filtered to have the same second order statistics as natural images. Experiments (following local guidelines) used a 2-alternative-forced-choice procedure in which the observer had to indicate which interval showed the base stimulus combined with contrast increment, as opposed to the base alone. The base stimulus was the full sized photograph, measuring 6 deg × 6 deg. The increment was a small, central, Gaussian-weighted patch of the photograph. Simultaneous staircases adjusted increment contrast for 8 base contrast values; performance converged on the 75 % correct, threshold rate.

For all 4 stimulus images, and for both observers, the plot of threshold increment contrast against base contrast showed both facilitation at low contrasts and high-contrast masking, but the amount of facilitation was less than obtained when we used sinusoidal gratings as base and increment. Facilitation was greatest for the random dot images, with discrimination threshold falling 8.0 dB below detection threshold for one observer, 6.0 dB for the other. Of the photographs, a street scene produced more facilitation than a garden scene (7.0 *vs.* 2.5dB for one observer, 4.5 *vs.* 3.5 dB for the other).

These data were compared with the predictions of a simple-cell computer model, based on the model of Foley (1994) and first developed for contrast discrimination experiments using sinusoidal stimuli. Good fits are achieved for the photograph experiments, but the model consistently underestimates the amount of facilitation that occurs in the random dot experiments. The results of the psychophysical and computational study suggest that similar neuronal mechanisms underlie the processing of contrast differences in sinusoidal and natural stimuli, and that understanding the experiments using sinusoidal stimuli can indeed shed some light on the processing of natural images. However, the differences between the data for the photographs and random dot images suggest that the natural scene data cannot be explained by reference to second-order statistics alone.

Foley J (1994). *J Opt Soc Am A* **11**, 1710–1719.

This work was supported by the MRC

All procedures accord with current local guidelines and the Declaration of Helsinki

C164

A Poisson decoder performs near-optimally at extracting motion signals from the temporally structured onset transients of MT neurons

Simon R. Schultz*† and J. Anthony Movshon *

**Center for Neural Science, New York University, NY, USA and †Wolfson Institute for Biomedical Research, UCL, London, UK*

Neurons in cortical area MT respond to step changes in visual motion with a transient pulse of high firing rate activity before settling down to their sustained level of response (Lisberger & Movshon 1999). These onset transients, unlike the sustained response, show fine-grained temporal structure.

To investigate MT transient dynamics, we recorded extracellularly from area MT of anaesthetised macaque monkeys using methods described in detail in (Kohn & Movshon, 2003). After induction with Ketamine HCl (10 mg kg^{-1}), anaesthesia was continued during surgery with 1.5–3.5 % isoflurane in a 98 % O_2/2 % CO_2 mixture. Experiments typically lasted 4–5 days, during which anaesthesia and neuromuscular blockade were maintained with sufentanil citrate (4–8 μg kg^{-1} h^{-1}) and vecuronium bromide (0.1 mg kg^{-1} h^{-1}) in Ringer's solution containing dextrose (2.5 %). Experiments conformed to local and national guidelines. The adequacy of anaesthesia was monitored continuously (EEG, ECG etc., see Kohn & Movshon (2003) for further details). Animals were humanely killed at the end of experiments.

Using an information theoretic approach (Panzeri & Schultz 2001), we found that the temporal structure in the onset transients can lead to either synergy or redundancy in the information content of spikes nearby in time, with a large variation from cell to cell. However, not all encoded information may be useful, so we compared the amount of information encoded about motion direction with that extracted by two maximum likelihood (ML) decoding strategies. The first strategy utilised complete knowledge of the probability of responses (spike trains) given stimuli, as determined from a training dataset. The second strategy, which we refer to as Poisson decoding, ignored correlations, instead assuming all time bins to be conditionally independent, and the response probability therefore obtained by the product of the spike probability distributions at each point in time. Neither decoder necessarily extracted all of the encoded information, some of which must therefore relate to differences in responses to non-preferred stimuli. The Poisson decoder performed almost as well as the ideal ML decoder, indicating that temporal structure in the onset transients neither helps nor hinders the extraction of motion signals from the spike train.

An adaptive filter implementation of Poisson decoding can be made using such well known mechanisms as synaptic depression and postsynaptic gain control; its near-optimal performance, together with the ubiquity of transient responses, is suggestive of a general mechanism present at each level of visual processing.

Kohn A & Movshon JA (2003). *Neuron* **39**, 681–691.

Lisberger SG & Movshon JA (1999). *J Neurosci* **19**, 2224–2246.

Panzeri S & Schultz SR (2001). *Neural Computation* **13**, 1311–1349.

This work was supported by the Howard Hughes Medical Institute.

All procedures accord with current national and local guidelines

C165

Computer simulation of the effects of spike encoding on the representation of natural scene information in visual cortex

D.J. Tolhurst*, H. Bulstrode* and B. Willmore†

** Department of Physiology, Downing Street, Cambridge CB2 3EG, UK and †Psychology Department, UC Berkeley, CA 94720-1650, USA*

There is much interest in the way that information about natural scenes is encoded by the visual cortex (V1), whose code needs many more neurons to be effective than a well-designed artificial one; perhaps the V1 code has compensatory advantages, such as energetic ones. Theoretical studies generally model V1 neurons as if they perform arithmetic to the same immense precision as the computers that perform the simulations. The responses of real neurons are imprecise since they are quantised by spike encoding, but could V1 be more robust to quantisation than artificial codes?

We have simulated several model arrays of V1 neurons to see how they might encode the spatial information in 16x16 pixel fragments of photographs of natural scenes. We used a full 256-filter set of the Principal Components (PCA) of such fragments, a set of 256 Gabor-like filters (each like a simple-cell receptive field), and a highly redundant (but more realistic) set of 1364 Gabors. For each set, we calculated how each filter responded to 10000 image fragments, and then how well each fragment could be reconstructed from the responses, using the pseudoinverse of the filter set.

PCA is a complete code, and so reconstruction is perfect, at least to the high arithmetic precision of the computer. To simulate the effects of a simple spike-rate code for response magnitude, we quantised the calculated filter responses before performing the fragment reconstructions. For each degree of quantisation, the 256-Gabor set performed 10–30 times worse than the 256-PCA, but the 1364 Gabor set (with its many more filters) performed slightly better than PCA.For all sets, as the number of quantisation levels increased, reconstruction errors fell. However, once there were more than 50–200 quantisation levels, there was less marked improvement in fragment reconstruction. A real V1 neuron is unlikely to be able to generate 50–200 spikes in the time that an animal takes to identify a visual stimulus (say 50–200 ms), but it has been argued that human contrast coding requires the cooperation of populations of neurons, with a maximal net response of about 180 spikes (Chirimuuta *et al.* 2003).

To encode image fragments with the same fidelity as PCA, the Gabor sets needed more 'spikes'. They also required at least as many neurons, so both of the Gabor sets are less metabolically efficient than PCA (Attwell & Laughlin, 2001). V1 is thought to have a Gabor-like code, but its benefit does not seem to be in conferring an energetic advantage.

Attwell D & Laughlin SB (2001). *J Cerebr Blood F Met* **21**, 1133–1145.

Chirimuuta M *et al.* (2003). *J Opt Soc Am A* **20**, 1253–1260.

HB received a Rank Proze Studentship

C166

Preferences of inferotemporal cortex neurons for the form and for the colour of complex visual stimuli are separable and uncorrelated

Andrew M Derrington* Amanda Parker* and Bharathi Jagadeesh†

** School of Psychology, University Park, Nottingham, NG7 2RD UK and † Department of Physiology & Biophysics, RPRC, University of Washington, WA 98195, USA*

We used conventional techniques* (Jagadeesh *et al.* 2001) to record from neurons in the anterior inferotemporal cortex and superior temporal sulcus of two monkeys (*Macaca mulatta*) while they performed a delayed match to sample visual recognition memory task using computer-generated cartoon faces 1.8–2.9° in height. We wished to test the relationship between colour and form preferences.

Each trial began with the presentation of a fixation target. When the monkey had fixated within a 3° square window centred on the target, a sample face, selected at random from the training set, was presented at fixation for 300 msecs. After the sample was turned off, two faces, one identical to the sample, the other differing either in colour or in form (shape), were presented 5.4 degrees to the left of the fixation target, one 5.4 degrees above and the other 5.4 degrees below. The monkey's task was to wait until the fixation point was turned off and then to make a saccade to the face that was identical to the sample. Both monkeys performed 800–1500 trials per day of this task to earn their daily water. They consistently performed above 90 % correct using a new set of 8 or 16 faces each day.

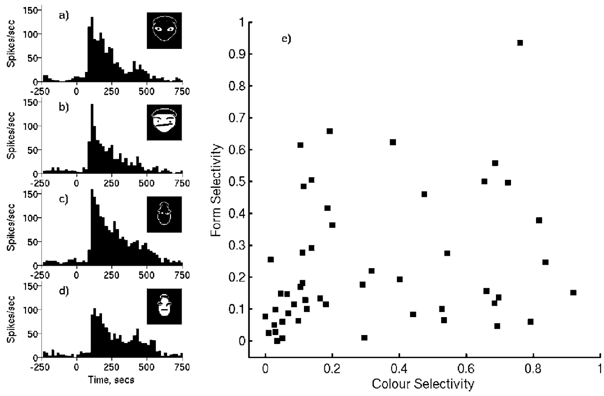

Figure 1. *a-d*, peristimulus time histograms showing responses measured during behavioural trials with the sample faces shown as insets; sample onset was at time 0. *e*, scatterplot of the absolute values of shape preference against colour preference.

Once a neuron had been isolated, a set of four faces (two different colours and two different shapes) was selected to test its preference for colour and shape. Responses to each face were measured by taking the peak firing rate, measured over 100 msecs, from the peristimulus time histogram (see Fig. 1*a–d*). Stimulus preferences (the difference between the responses to 2 stimuli divided by the sum) were measured, from the neurons (50 of 102 recorded) that gave incremental responses of at least 5 spikes/sec. Preferences for colour and for shape appeared to be separable: within each neuron colour preferences measured with different shapes were strongly correlated and vice versa. Selectivity for colour and for shape appeared to be independent. Figure 1*e* shows that there was no significant correlation between the degree of selectivity for the two attributes across the population of neurons recorded.

*Experimental protocols were approved by the University of Washington Animal Care and Use Committee and were consistent with UK legislation. Preparatory surgery was carried out under isoflurane anaesthesia followed by prophylactic pain relief and antibiotics at least 2 weeks prior to recording.

Jagadeesh B *et al.* (2001). *JNeurophysiol* **86**, 290–303.

This work was supported by:-BBSRC, Wellcome Trust, NIH, McKnight Foundation, Sloan Foundation, Whitehall Foundation

All procedures accord with current national and local guidelines

PC127

The effect of distractors on saccadic latency

H.I. Lamabadusuriya, R.I.R. Martin and R.H.S. Carpenter

The Physiological Laboratory, University of Cambridge, Cambridge CB2 3EG, UK

In the LATER model of saccadic and other latencies, neural decision signals rise, in response to information from a stimulus, from an initial level representing prior probability to a threshold at which action is initiated (Carpenter & Williams, 1995). When more than one target is presented, the decision signals race against one another, with a saccade being made to the winner. Neurophysiological and behavioural evidence suggests that such competing units inhibit one another, so that it takes longer to decide between two targets than it takes to make a saccade to one. A previous study using a countermanding task suggested that this competition may affect μ, the mean rate of rise of the decision signal across trials (Hanes and Carpenter, 1999). Here we test this prediction directly, presenting distractors at the same time as targets.

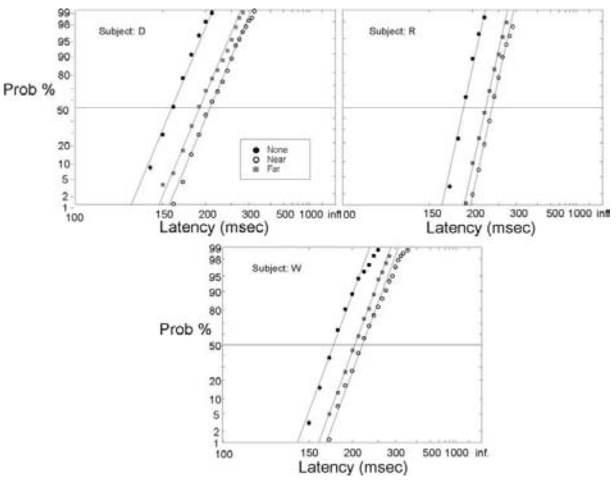

Figure 1. Cumulative saccadic latency distributions plotted on a probit scale as a function of reciprocal latency for three participants in paradigm 2. In each case, distributions are shown for trials with no distractor (control), and with contralateral near or far distractors, and have been fitted (Kolmogorov-Smirnov, $P > 20\%$) by sets of straight lines constrained to be parallel, as would be expected if in the LATER model the effect of distractors is to alter the mean rate of rise of the decision signal.

Saccadic eye movements were recorded, with informed consent and local ethical committee approval, from six participants in a step task. In control trials, subjects made a saccade to a green LED target presented randomly 3.7° to right or left of a central fixation LED, simultaneously extinguished. In test trials, randomly interleaved with the controls, the target was accompanied by a red distractor LED presented simultaneously at a different location. A participant typically performed around 2000 trials in an experiment. In one experiment (paradigm 1) distractors were presented either ipsilaterally or contralaterally at an eccentricity of 5.5°. In a second experiment (paradigm 2), distractors were always contralateral, either near (5.5°) or far (9.2°) from the fixation target. Saccadic latencies were measured and analysed. In paradigm 1, contralateral distractors increased latency by around 20–50 msec; ipsilateral distractors caused no significant increase in latency, but in 3 of the 6 subjects induced a small but significant (Student's unpaired t test, $P < 5\%$) decrease; similar differences have been reported by Walker *et al.* (1997). In paradigm 2, contralateral distractors increased latency, causing the distributions to move in a parallel fashion on reciprobit plots (Fig. 1): near distractors were more potent than far. Likelihood analysis showed an average support of 55.6 per subject across both experiments and all subjects for the hypothesis that, in terms of the LATER model, distractors do indeed affect the mean rate of rise of the decision signal rather than its starting point.

Carpenter RHS & Williams MLL (1995). *Nature* **377**, 59–62.

Hanes DP & Carpenter RHS (1999). *Vison Research* **39**, 2777–2791.

Walker R *et al.* (1997). *J Neurophysiol* **78**, 1096–1107.

All procedures accord with current local guidelines and the Declaration of Helsinki

PC128

Chloride transport by the guinea pig outer hair cell membrane investigated by the anion sensitive dye MEQ

Ione Harding, Nathan Thevathasan and Jonathan Ashmore

Department of Physiology and Centre for Auditory Research, UCL, Gower Street, London WC1E 6BT, UK

The electromotility of outer hair cells (OHCs) in the organ of Corti allows enhanced sensitivity and frequency selectivity in mammalian hearing. There is good evidence that voltage sensitive motor complex, localised in the basolateral membrane and containing a novel motor protein' prestin', is responsible for this phenomenon. Prestin is a member of a superfamily (SLC26) of anion-bicarbonate exchangers which are expressed in a wide range if tissues. We have investigated the transport of chloride by prestin chloride indicator 6-Methoxy-N-ethylquinolinium iodide (MEQ, Molecular Probes). As a voltage dependant motor intracellular anions are thought to act as the sensor (Oliver *et al.* 2001).

OHCs were isolated from the cochlea of the guinea pig following humane cervical dislocation. Cells were bathed in hepes buffered perilymph containing (mM): Cl, 155; Na, 144; K, 4.6; Mg, 1.5; Ca, 1.5; hepes, 5; pH 7.3, 320 mOsm. MEQ (3 mM) was loaded into the cells via the patch pipette using conventional intracellular medium containing 30 mM KCl and gluconate as the substitute anion. The intracellular fluorescent dye is reversibly quenched by chloride. Using *in vitro* calibration, we estimate the IC_{50} for Cl quench to have been 8.7 mM. MEQ quench was virtually independent of gluconate (IC_{50}, 200 mM). When cells were voltage clamped at −40 mV and equilibrated with MEQ, the imaged fluorescence levels increased when an extracellular solution containing 0 Cl (gluconate as substituting anion) was perfused around the OHC lateral membrane, indicating a reduction of intracellular chloride. Simultaneous recordings showed a small increase in outward current through the cell membrane. Cells shortened by about 4 % as the volume increased. The increase in fluorescence was not due to an increase in illumination path length as fluorescence changes also occurred in cells collapsed by hypo-osmotic intracellular solution. Salicylate, known to block electromotility, eliminated ionic current changes on zero chloride solution exposure suggesting chloride is transported through the prestin motor complex. The data is consistent with prestin being a low efficacy integral membrane transporter whose motor function is a consequence of the anion transport cycle.

Oliver D *et al.* (2001). *Science* **292**, 2340–2343.

This work was supported by the Wellcome Trust. NT held a vacation studentship of the Physiological Society.

All procedures accord with current UK legislation

PC129

Motion adaptation does not affect the direction tuning of a neuron processing optic flow in the blowfly *Calliphora vicina*

G. Card, H.G. Krapp and Simon B. Laughlin

Department of Zoology, University of Cambridge, Downing Street, Cambridge CB2 3EJ, UK

Adaptation adjusts a neuron's operating range to its input. When sensory systems use population codes, selective adaptation of a subset of neurons could corrupt coding. To see how adaptation influences the coding of optic flow we recorded from motion-sensitive Tangential Neurons (TNs) in the lobula plate of the blowfly *Calliphora vicina*.

Each TN's receptive field is matched to the pattern of optic flow induced by a certain rotation or translation. A population of about 50 TNs codes information on ego-motion the fly uses for flight and gaze stabilisation. The matched receptive field of a TN is formed by combining inputs from Elementary Motion Detectors (EMDs) aligned along the 3 axes of the hexagonal sampling lattice of the compound eye (Krapp *et al.* 1998). To monitor the horizontal motion induced by yaw the spiking Tangential Neuron H1 combines inputs from two sets of EMDs, aligned at +30 degrees and −30 degrees to the horizontal. We investigated whether adaptation of H1 to motion in one direction alters the directional tuning of its receptive field.Extracellular recordings were made from the lobula plate of 4 restrained and un-anaesthetised blowflies. We used the rotating dot method (Krapp and Hengstenberg, 1997) to measure the directional tuning of a small region of H1's receptive field immediately before and after a 5 s presentation of an adapting grating. The determination of directional sensitivity took less than 1s. The adapting grating (contrast>90 %; contrast frequency 12 Hz, spatial wavelength 5 degrees) reduced H1's response by 50 %. The grating was oriented at 45 to the horizontal to selectively stimulate one set of EMDs. A linear model of directionally selective adaptation of EMDs predicted that this grating should shift H1's preferred direction of motion by approximately 10°. However, local mapping of H1's receptive field failed to find a statistically significant shift in directional sensitivity (Student's unpaired *t* test, $n = 40$, $P < 0.1$). Changing the direction and contrast frequency of the adapting stimulus did not change this finding.

Our results show that strong adaptation to motion in one direction does not distort the receptive field of H1. This suggests that adaptation in H1 is dominated by the non-directional mechanism (Harris *et al.* 2000). The use of non-directional adaptation to preserve receptive field structure is an important prerequisite for the coding of self-motion by a population of neurons.

Harris RA *et al* (2000). *Neuron* **28**, 595–606.

Krapp HG & Hengstenberg R (1997). *Vis Res* **37**, 225–234.

Krapp HG *et al* (1998). *J Neurophysiol* **79**, 1902–1917.

This work was supported by the CT Taylor Fund (GC), the Royal Soc (HGK), and the Rank Price Fund (SBL)

PC130

Receptive field organisation of a collision-detecting visual interneurone in solitarious and gregarious locusts

S.M. Rogers, G.W.J. Harston, F. Kilburn-Toppin, T. Matheson and H.G. Krapp

Department of Zoology, Univ. of Cambridge, Downing Street, Cambridge CB2 3EJ, UK

Locusts *Schistocerca gregaria* take on a range of forms between two morphologically and behaviourally distinct extremes, the solitarious and gregarious phases. An identified visual interneurone, the descending contralateral movement detector (DCMD), has different response properties in the two phases (Matheson *et al.* 2003), which may be related to known differences in visually mediated behaviours. DCMD responds maximally to objects looming on a direct collision course. During flight or walking, most looming objects will appear in the frontal visual field as the animal moves forwards. When the locust is stationary on the ground, predators could approach from any direction. We tested the responses of DCMD to objects looming from different angular positions within the visual field.

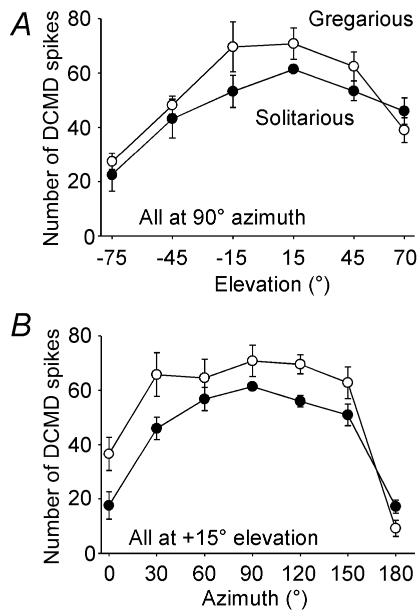

Figure 1. The number of spikes per approach differed across elevation (A) and azimuth (B) for both gregarious (open symbols) and solitarious (filled symbols) locusts. The tuning curves of the two phases differed most strongly in the frontal field just above the horizon. $n = 5$ solitarious, 5 gregarious. Mean ± S.D.

DCMD in gregarious locusts (Fig. 1A) was excited more strongly by objects that approached from just above or below the horizontal plane (−15° to +15° elevation) than by objects that approached from ± 45 or ± 70°. For objects approaching at an elevation of +15° or −15° the sensitivity of DCMD was maintained for azimuths of 30–150° but fell off for angles of 0° and 180°, where 0° is straight ahead (Fig. 1B). DCMD in solitarious locusts generally responded with fewer spikes per approach than did DCMD of gregarious animals (Fig. 1A, B). The difference between phases was greatest for elevations of +15° and −15°, so that the tuning curve (in elevation) of solitarious animals was flatter than that for gregarious animals (Fig. 1A). The greatest relative difference in number of spikes per approach was at azimuth 0°, where DCMD of solitarious locusts produced 18 spikes and DCMD of gregarious locusts produced 37 spikes (Fig. 1B; a difference of 206 %). Overall, there was a significant effect of phase on number of spikes per approach across the visual field (GLM, $F_{1, 222} = 5.34$, $P = 0.022$). DCMD of gregarious locusts is relatively more sensitive than DCMD of solitarious locusts to objects looming from just above the horizon, particularly on a frontal trajectory. This difference may reflect adaptation to different behaviourally relevant stimuli. It may permit gregarious locusts to better avoid collisions when flying in swarms or marching in bands.

Matheson T *et al.* (2003). *J Neurophysiol* DOI 10.1152/jn.00795

This work was supported by the BBSRC.